The Neutrino Response of Low-Density Neutron Matter from the Virial Expansion

C.J. Horowitz[1,*] and A. Schwenk[2,†]
[1]Nuclear Theory Center and Department of Physics, Indiana University, Bloomington, IN 47408
[2]Department of Physics, University of Washington, Seattle, WA 98195-1560

We generalize our virial approach to study spin-polarized neutron matter and the consistent neutrino response at low densities. In the long-wavelength limit, the virial expansion makes model-independent predictions for the density and spin response, based only on nucleon-nucleon scattering data. Our results for the neutrino response provide constraints for random-phase approximation or other model calculations, and we compare the virial vector and axial response to response functions used in supernova simulations. The virial expansion is suitable to describe matter near the supernova neutrinosphere, and this work extends the virial equation of state to predict neutrino interactions in neutron matter.

PACS numbers: 21.65.+f, 26.50.+x, 25.30.Pt, 97.60.Bw
Keywords: Low-density neutron matter, neutral-current neutrino scattering, virial expansion

I. INTRODUCTION

Neutrinos radiate 99% of the energy in core-collapse supernovae. The scattering of neutrinos and the physics of the explosion are most sensitive to the properties of low-density nucleonic matter [1, 2], which is a complex problem due to strong coupling with large scattering lengths, clustering in nuclear matter and the non-central nature of nuclear interactions. For low densities and high temperatures, the virial expansion provides a tractable approach to strong interactions, and in previous works we have presented the virial equation of state of low-density nucleonic matter [3, 4]. The predicted large symmetry energy at low densities has been confirmed in near Fermi energy heavy-ion collisions [5].

The virial approach can be used to describe matter in thermal equilibrium around the neutrinosphere in supernovae. The temperature of the neutrinosphere is roughly $T \sim 4\,\mathrm{MeV}$ from about 20 neutrinos detected in SN1987a [6, 7], and the density follows from known cross sections of neutrinos with these energies $n \sim 10^{11} - 10^{12}\,\mathrm{g/cm^3}$. For neutron matter, the virial expansion in terms of the fugacity $z = e^{\mu/T}$ is valid for

$$n = \frac{2}{\lambda^3}\, z + \mathcal{O}(z^2) \lesssim 4 \cdot 10^{11}\,(T/\mathrm{MeV})^{3/2}\,\mathrm{g/cm^3}\,, \quad (1)$$

where we require $z < 1/2$ and λ denotes the thermal wavelength $\lambda = (2\pi/mT)^{1/2}$. Therefore, the virial approach makes model-independent predictions for the conditions of the neutrinosphere, based only on the experimental scattering data.

In this paper, we use the virial expansion to describe how neutrinos interact with low-density neutron matter. We focus on neutral-current interactions, and leave charged-current reactions and nuclear matter to future works. Our long-term goal is a reliable equation of state and consistent neutrino response for supernovae.

The free cross section per particle for neutrino-neutron elastic scattering is given by [8]

$$\frac{1}{N}\frac{d\sigma_0}{d\Omega} = \frac{G_{\mathrm{F}}^2 E_\nu^2}{4\pi^2}\biggl(C_a^2\,(3-\cos\theta) + C_v^2\,(1+\cos\theta)\biggr)\,, \quad (2)$$

where G_{F} is the Fermi coupling constant, E_ν the neutrino energy, and θ the scattering angle. The weak axial coupling is $C_a = g_a/2$, with $g_a = 1.26$ the axial charge of the nucleon. The weak vector charge is $C_v = -1/2$ for scattering from a neutron. Eq. (2) neglects corrections of order E_ν/m from weak magnetism and other effects [9].

In the medium, this cross section is modified by the vector response $S_v(q)$ and the axial response $S_a(q)$

$$\frac{1}{N}\frac{d\sigma}{d\Omega} = \frac{G_{\mathrm{F}}^2 E_\nu^2}{16\pi^2}\biggl(g_a^2\,(3-\cos\theta) S_a(q) + (1+\cos\theta) S_v(q)\biggr)\,, \quad (3)$$

where S_v and S_a describe the response of the system to density and spin fluctuations respectively, and $q = 2E_\nu \sin(\theta/2)$ denotes the momentum transfer. We will discuss the approximations for Eq. (3) in Sect. II C. In the following, we will use the virial expansion to provide model-independent results for the response in the long-wavelength ($q \to 0$) or forward-scattering limit.

This paper is organized as follows. We extend the virial equation of state to spin-polarized matter in Section II and derive the consistent long-wavelength response. Further details on the virial equation of state can be found in Refs. [3, 4]. In Section III, we present results for the spin virial coefficients, the pressure and entropy of spin-polarized neutron matter, and the neutrino response. We compare our results to Brueckner calculations, and to random-phase approximation (RPA) response functions. Finally, we conclude in Section IV.

*E-mail: horowit@indiana.edu
†E-mail: schwenk@u.washington.edu

II. FORMALISM

The virial expansion is a general, model-independent approach for a dilute gas, provided the fugacity is small and for temperatures above any phase transitions. Under these conditions, the grand-canonical partition function can be expanded in powers of the fugacity. The second virial coefficient b_2 describes the z^2 term in this expansion and is directly related to the two-body scattering phase shifts [10, 11]. The relation of the third virial coefficient to three-body scattering is not straightforward, and was only studied for special cases [12, 13, 14]. The virial expansion is not a perturbative $k_{\rm F} a_s$ expansion, and its great advantage is that it includes bound states and scattering resonances on an equal footing.

A. Spin-Polarized Matter

The virial equation of state is easily generalized to spin-asymmetric systems. For two spin components, we denote the chemical potential for spin up and spin down particles by μ_+ and μ_-, with fugacity $z_+ = e^{\mu_+/T}$ and $z_- = e^{\mu_-/T}$ respectively. For the virial equation of state we expand the pressure in a power series of the fugacities

$$P = \frac{T}{\lambda^3}\bigl(z_+ + z_- + b_{n,1}\,(z_+^2 + z_-^2) + 2\,b_{n,0}\,z_+ z_- + \mathcal{O}(z^3)\bigr)\,. \tag{4}$$

The second virial coefficients $b_{n,1}$ for like spins and $b_{n,0}$ for opposite spins are related to the two-particle partition function and are given in terms of the scattering phase shifts in the next section. The densities follow from differentiating the pressure with respect to the fugacities. For the density of spin-up neutrons $n_+ = (\partial_{\mu_+} P)_T = z_+/T\,(\partial_{z_+} P)_T$ we thus have

$$n_+ = \frac{1}{\lambda^3}\bigl(z_+ + 2\,b_{n,1}\,z_+^2 + 2\,b_{n,0}\,z_+ z_- + \mathcal{O}(z^3)\bigr)\,, \tag{5}$$

and likewise for the density n_- of spin-down neutrons

$$n_- = \frac{1}{\lambda^3}\bigl(z_- + 2\,b_{n,1}\,z_-^2 + 2\,b_{n,0}\,z_- z_+ + \mathcal{O}(z^3)\bigr)\,. \tag{6}$$

The total density n and the spin polarization Δ are then given by

$$n = n_+ + n_- \quad \text{and} \quad \Delta = \frac{n_+ - n_-}{n_+ + n_-}\,. \tag{7}$$

In this work, we truncate the virial expansion after second order in the fugacities. This leads to an equation of state that is thermodynamically consistent.

The dependence of the total density and the spin polarization on z_+ and z_- can be inverted to yield the virial equation of state directly in terms of $P\bigl(z_+(n,\Delta,T), z_-(n,\Delta,T), T\bigr)$. In practice, for a given spin polarization, we determine the spin-down fugacity as a function of the spin-up one $z_-(z_+,\Delta,T)$, and generate the virial equation of state in tabular form for a range of z_+ values. This maintains the thermodynamic consistency of the virial equation of state.

Finally, we will also discuss results for the entropy. The entropy density $s = S/V$ follows from differentiating the pressure with respect to the temperature $s = (\partial_T P)_{\mu_i}$. This leads to

$$\begin{aligned} s = {}& \frac{5P}{2T} - n_+ \log z_+ - n_- \log z_- \\ & + \frac{T}{\lambda^3}\bigl(b'_{n,1}\,(z_+^2 + z_-^2) + 2\,b'_{n,0}\,z_+ z_-\bigr)\,, \end{aligned} \tag{8}$$

where $b'(T) = db(T)/dT$ denotes the temperature derivative of the virial coefficients.

B. Spin Virial Coefficients

The second virial coefficient $b_{n,1}$ describes the interaction of two neutrons with the same spin projection. To this end, we generalize the second virial coefficient of the spin-symmetric system [4, 10, 11] to

$$b_{n,1}(T) = \frac{2^{1/2}}{\pi T}\int_0^\infty dE\, e^{-E/2T}\,\delta_1^{\rm tot}(E) - 2^{-5/2}\,, \tag{9}$$

where $-2^{-5/2}$ is the free Fermi gas contribution and $\delta_1^{\rm tot}(E)$ is the sum of the isospin and spin-triplet elastic scattering phase shifts at laboratory energy E. This sum is over all partial waves with angular momentum L and total angular momentum J allowed by spin statistics, and includes a degeneracy factor $(2J+1)/(2S+1)$,

$$\begin{aligned} \delta_1^{\rm tot}(E) &= \sum_{L,J} \frac{2J+1}{3}\,\delta_{^3{\rm L}_J}(E) \\ &= \frac{1}{3}\,\delta_{^3{\rm P}_0} + \delta_{^3{\rm P}_1} + \frac{5}{3}\,\delta_{^3{\rm P}_2} + \ldots \end{aligned} \tag{10}$$

The factor $1/(2S+1) = 1/3$ arises because the same spin projection, e.g., for up spins $M_S = +1$, is 1/3 of the possibilities $M_S = -1, 0, 1$. Note that we have neglected the effects of the mixing parameters due to the tensor force. We expect that their contributions are small for low densities.

Two neutrons with opposite spin projections have a probability 1/2 to be in spin $S = 0$ or $S = 1$ states, thus the second virial coefficient for opposite spins $b_{n,0}$ is given by

$$b_{n,0}(T) = \frac{2^{1/2}}{\pi T}\int_0^\infty dE\, e^{-E/2T}\,\delta_0^{\rm tot}(E)\,, \tag{11}$$

where $\delta_0^{\rm tot}(E)$ is the sum of allowed isospin-triplet elastic scattering phase shifts with degeneracy factor $(2J +$

1)/(2(2S + 1)),

$$\delta_0^{\rm tot}(E) = \sum_{S,L,J} \frac{2J+1}{2(2S+1)}\,\delta_{^{2S+1}{\rm L}_J}(E)$$
$$= \frac{1}{2}\,\delta_{^1{\rm S}_0} + \frac{1}{6}\,\delta_{^3{\rm P}_0} + \frac{1}{2}\,\delta_{^3{\rm P}_1} + \frac{5}{6}\,\delta_{^3{\rm P}_2} + \frac{5}{2}\,\delta_{^1{\rm D}_2} + \ldots \tag{12}$$

The second virial coefficient for spin-symmetric neutron matter b_n is the sum over like and opposite spins,

$$b_n = b_{n,1} + b_{n,0}\,, \tag{13}$$

and consequently the sum of the total phase shifts given above determines b_n with $\delta^{\rm tot}(E)/2 = \delta_0^{\rm tot}(E) + \delta_1^{\rm tot}(E)$ [29]. In addition, we define the axial spin virial coefficient b_a as

$$b_a = b_{n,1} - b_{n,0}\,. \tag{14}$$

Thus, if only S-wave interactions are present, one has

$$b_{n,1} = -2^{-5/2} \quad \text{and} \quad b_a = -b_n - 2^{-3/2}\,. \tag{15}$$

C. Neutrino Response

Neutrino scattering from a many-body system can be expressed in terms of the vector $S_v(q,w)$ and axial $S_a(q,w)$ dynamical response functions. These describe the probability for a neutrino to transfer momentum q and energy w to the medium. Integrating over energy transfer, we define the static vector $S_v(q)$ and axial $S_a(q)$ response functions

$$S_{v,a}(q) = \int_{-q}^{q} dw\, S_{v,a}(q,w)\,. \tag{16}$$

Here scattering kinematics limits the energy transfer to be space-like $|w| < q$. At low densities nucleons are non-relativistic, and therefore we expect the vector response to have little strength in the time-like region so that

$$S_v(q) \approx \int_{-\infty}^{\infty} dw\, S_v(q,w)\,. \tag{17}$$

The axial response can have contributions from multi-pair states in the time-like region even in the long-wavelength limit due to non-central nuclear interactions [15]. However, neutron matter at very low density can be described using a pion-less effective field theory where non-central interactions are sub-leading. Therefore, in this paper we approximate the axial response by

$$S_a(q) \approx \int_{-\infty}^{\infty} dw\, S_a(q,w)\,. \tag{18}$$

The static structure factor for the density response is then given by

$$n\,S_v(q) = \frac{1}{Z}\sum_j e^{-\beta E_j} \int d^3\mathbf{r}\; e^{i\mathbf{q}\cdot\mathbf{r}} \times \langle j|\psi^\dagger(\mathbf{r})\psi(\mathbf{r})\psi^\dagger(0)\psi(0)|j\rangle\,, \tag{19}$$

where the sum is over all many-body eigenstates $|j\rangle$ with energy E_j, the partition function is $Z = \sum_j e^{-\beta E_j}$ and $\beta = 1/T$. For the spin response, the density operator is replaced by the spin density $\psi^\dagger(\mathbf{r})\boldsymbol{\sigma}\psi(\mathbf{r})$.

In the long-wavelength limit, the vector response of the spin-symmetric system is given by [16] (see also Appendix B in [17])

$$S_v(q=0) = \frac{T}{(\partial P/\partial n)_T}\,. \tag{20}$$

For the symmetric system, the total chemical potential is $\mu = (\mu_+ + \mu_-)/2$, with fugacity $z = \sqrt{z_+ z_-} = e^{\mu/T}$, and the virial equation of state (see also Ref. [4]) yields for the consistent vector response,

$$S_v(q=0) = \frac{z}{n}\left(\frac{\partial n}{\partial z}\right)_T = \frac{1+4b_n z}{1+2b_n z}\,. \tag{21}$$

Following Burrows and Sawyer [17], we define the spin-difference or axial chemical potential $\mu_a = (\mu_+ - \mu_-)/2$ and the axial fugacity $z_a = \sqrt{z_+/z_-}$. The axial response of the spin-symmetric system is then given by

$$S_a(q=0) = \frac{z_a}{n}\frac{\partial}{\partial z_a}(n_+ - n_-)\bigg|_{z_a=1}\,, \tag{22}$$

and the virial expansion, Eq. (4), leads to

$$S_a(q=0) = 1 + \frac{2b_a z}{1+2b_n z}\,. \tag{23}$$

The long-wavelength limit of the axial response is also related to the spin susceptibility χ,

$$S_a(q=0) = \frac{\chi}{\chi_{\rm F}} = \frac{nT}{(\partial^2 f/\partial\Delta^2)_{n,T,\Delta=0}}\,, \tag{24}$$

where f denotes the free energy density, and $\chi_{\rm F} = \mu_n^2 n/T$ is the spin susceptibility of a free neutron gas, with the neutron magnetic moment μ_n. Finally, the response functions are normalized to unity in the low-density limit $S_v(0) = S_a(0) = 1$ for $z = n = 0$.

III. RESULTS

A. Spin Virial Coefficients

We first calculate the virial coefficients b_n and b_a from the $T = 1$ np phase shifts obtained from the Nijmegen

TABLE I: The second virial coefficient b_n and the axial virial coefficient b_a for different temperatures. The results labeled CIB take into account the effects due to charge-independence breaking (CIB) on the scattering length with $a_{nn} = -18.5$ fm. We estimated an error of $< 5\%$ for the higher temperatures $T \geqslant 25$ MeV due to the truncation of the integration over the phase shifts at $E \leqslant 350$ MeV.

T[MeV]	b_n	with CIB	$T\,b'_n$	b_a	with CIB	$T\,b'_a$
1.00	0.288	0.251	0.032	-0.641	-0.604	-0.031
2.00	0.303	0.273	0.012	-0.655	-0.625	-0.007
3.00	0.306	0.279	0.004	-0.655	-0.629	0.006
4.00	0.306	0.283	0.001	-0.652	-0.628	0.014
5.00	0.306	0.285	0.000	-0.648	-0.627	0.020
6.00	0.306	0.286	0.001	-0.644	-0.624	0.023
7.00	0.307	0.288	0.002	-0.640	-0.621	0.026
8.00	0.307	0.289	0.004	-0.637	-0.619	0.028
9.00	0.308	0.291	0.007	-0.634	-0.616	0.029
10.00	0.309	0.292	0.009	-0.631	-0.614	0.029
12.00	0.310	0.295	0.013	-0.625	-0.610	0.029
14.00	0.313	0.299	0.017	-0.621	-0.607	0.028
16.00	0.315	0.302	0.020	-0.617	-0.604	0.026
18.00	0.318	0.305	0.022	-0.614	-0.602	0.024
20.00	0.320	0.308	0.023	-0.612	-0.600	0.021
22.00	0.322	0.311	0.023	-0.610	-0.598	0.019
24.00	0.324	0.313	0.022	-0.608	-0.597	0.018
26.00	0.326	0.315	0.021	-0.607	-0.596	0.017
28.00	0.327	0.317	0.018	-0.606	-0.595	0.016
30.00	0.329	0.318	0.015	-0.605	-0.595	0.016
35.00	0.330	0.321	0.004	-0.602	-0.593	0.018
40.00	0.330	0.321	-0.009	-0.599	-0.591	0.024
45.00	0.328	0.319	-0.025	-0.596	-0.588	0.031
50.00	0.324	0.316	-0.041	-0.592	-0.584	0.041

partial wave analysis [18]. This neglects the small charge dependences in nuclear interactions. We have included all partial waves with $L \leqslant 6$. For the higher temperatures, $T \geqslant 25$ MeV, there is a $< 5\%$ error due to the truncation of the integration over the phase shifts at $E \leqslant 350$ MeV (the extent of the partial wave analysis). This error was estimated by assuming constant total phase shifts and varying the energy cutoff to $E > 350$ MeV.

Our results for the virial coefficients and their temperature derivatives $Tb'(T)$ are listed in Table I. As discussed in Ref. [4], the virial coefficients are dominated by the large S-wave scattering length physics ($a_{np} = -23.768$ fm and $a_{nn} = -18.5$ fm), but effective range and higher partial wave contributions are noticeable. For example, for $T = 5$ MeV, the virial coefficients obtained only from a_{np} are $b_n = 0.44$ [4] and $b_a = -b_n - 2^{-3/2} = -0.80$. In the unitary limit where the scattering length $|a_s| = \pm\infty$ and $\delta(E) = \pi/2$, the second virial coefficients are independent of the temperature and given by $b_n = 3/2^{5/2} = 0.53$ [19]

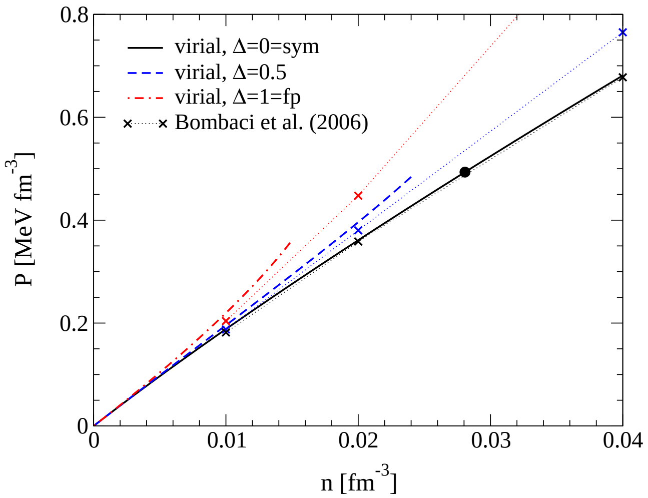

FIG. 1: (Color online) The pressure P versus density n for $T = 20$ MeV and various spin polarizations $\Delta = 0$ (symmetric), 0.5 and 1 (fully polarized). We also compare our results to Brueckner calculations of Bombaci *et al.* (crosses with dotted lines) [23] for $\Delta = 1, 0.5, 0$ (top to bottom). The circle indicates where the fugacity is $z = 0.5$ for $\Delta = 0$, and for the other spin polarizations the virial curves end at $z = 1$.

and $b_a = -5/2^{5/2} = -0.88$. Therefore, the virial expansion is well defined for resonant interactions, in contrast to the $k_{\rm F} a_s$ expansion.

We find that the second virial coefficients are approximately independent of temperature over a wide range, and consequently $Tb'(T) \approx 0$. As a result, the thermodynamic properties of spin-polarized neutron matter and the long-wavelength response scale as a function of the fugacities, which depend on density and temperature through $z_i(n_+/T^{3/2}, n_-/T^{3/2})$ for $i = +$ and $i = -$. This scaling can also be expressed in terms of the Fermi temperatures $T_{{\rm F},i} \sim n_i^{2/3}$, and thus the properties of neutron matter scale with $T/T_{{\rm F},i} \sim T/n_i^{2/3}$ only. In Ref. [4] we found that spin-symmetric neutron matter scales to a very good approximation. The virial scaling symmetry is exact for cold atomic gases tuned to a Feshbach resonance [20] and has been verified experimentally by Thomas *et al.* [21].

In Table I, we also study the effects of charge-independence breaking (CIB) on the scattering length. We estimate CIB effects as discussed in Ref. [4]. CIB for the virial coefficients is largest for $T < 5$ MeV and leads to a 10% reduction in magnitude of the virial coefficients.

B. Pressure and Entropy of Spin-Polarized Matter

We have previously found [4] good agreement of the virial equation of state for spin-symmetric neutron matter with microscopic Fermi hyper-netted chain (FHNC) calculations of Friedman and Pandharipande [22] for densities up to $n \lesssim n_0/10$, where $n_0 = 0.16\,{\rm fm}^{-3}$ is the sat-

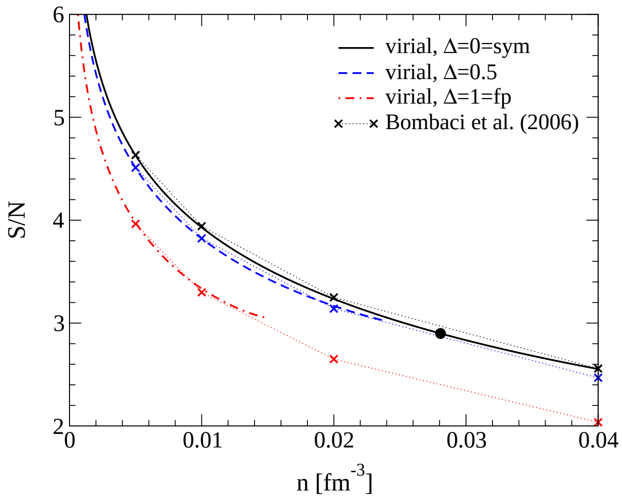

FIG. 2: (Color online) The entropy per particle S/N versus density n for $T = 20\,\text{MeV}$ and various spin polarizations $\Delta = 0$ (symmetric), 0.5 and 1 (fully polarized). We also compare our results to Brueckner calculations of Bombaci *et al.* (crosses with dotted lines) [23] for $\Delta = 0, 0.5, 1$ (top to bottom). The circle indicates where the fugacity is $z = 0.5$ for $\Delta = 0$, and for the other spin polarizations the virial curves end at $z = 1$.

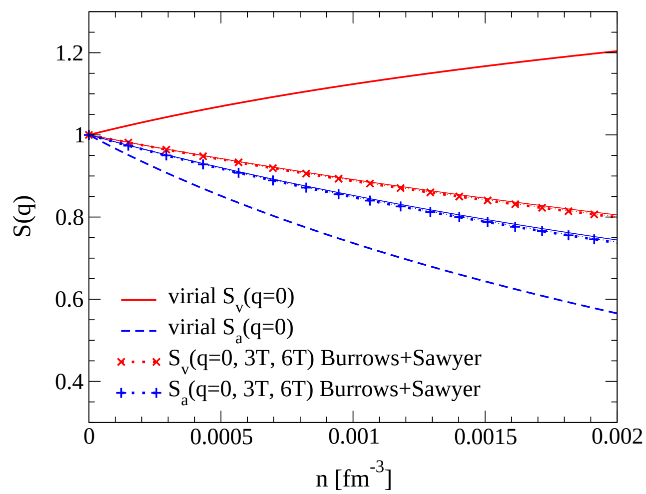

FIG. 3: (Color online) The vector and axial response of neutron matter for $T = 4\,\text{MeV}$. In addition to the long-wavelength virial response, we also show the RPA response of Burrows and Sawyer [17] for neutron matter and various momentum transfers $q = 0, 3T$ and $6T$. For this density range, the fugacity in the virial expansion is $z < 0.42$.

uration density of symmetric nuclear matter, and published temperatures $T \geqslant 10\,\text{MeV}$. For nuclear matter, the FHNC results fail to describe clustering with alpha particles at low densities [3].

Our virial results for the pressure and entropy of spin-polarized neutron matter are shown in Figs. 1 and 2 for $T = 20\,\text{MeV}$ and polarizations $\Delta = 0$ (symmetric), 0.5 and 1 (fully polarized). For this temperature, we can compare the virial results to Brueckner calculations of Bombaci *et al.* [23]. As shown in Fig. 2, the Brueckner entropy agrees well with the virial results. For the pressure, the effects of a spin polarization are smaller, and in addition there is some uncertainty in the Brueckner calculations, since the pressure was obtained from the energy by a numerical derivative. Before we discuss the neutrino response, we note that it is difficult to calculate the long-wavelength response at low densities from the Brueckner or FHNC results, since the response is obtained by differentiating the pressure.

C. Neutrino Response

Our virial results for the long-wavelength vector and axial response are presented in Fig. 3. The neutron-neutron interaction is attractive at long distances and thus increases the probability to find two neutrons close together compared to a free neutron gas. These density fluctuations increase the local weak charge and produce a vector response $S_v > 1$ for low-momentum transfers. This is easily seen by expanding the vector response to lowest order in the density. With $z \approx n\lambda^3/2$, we have

$$S_v(q=0) \approx 1 + b_n n\lambda^3 > 1\,, \tag{25}$$

since $b_n = 0.31$ from Table I. In a Landau-Fermi liquid, the vector response is given by $S_v(0) = 1/(1+F_0) > 1$ for neutron matter, where the Landau parameter for the density-density interaction is $F_0 < 0$ [24].

In contrast, the spin-spin interaction is repulsive (this follows from the Pauli principle, when the density-density interaction is attractive), and the virial axial response gives $S_a < 1$ for low-momentum transfers. This is seen in the low-density limit,

$$S_a(q=0) \approx 1 + b_a n\lambda^3 < 1\,, \tag{26}$$

where $b_a = -0.65$ from Table I. Analogous to the vector response, the axial response for a Landau-Fermi liquid is given by $S_a(0) = 1/(1+G_0) < 1$ for neutron matter, since the Landau parameter for the spin-spin interaction is $G_0 > 0$ [24]. Although the virial densities and temperatures are not in a Fermi liquid regime ($z \sim (T_{\rm F}/T)^{3/2} \ll 1$), the deviation of the vector and axial response from a free gas is determined by nuclear interactions, and thus is the same for low and high temperatures.

D. Comparison to RPA calculations

Most present calculations of the neutrino response are based on the random-phase approximation (RPA) [2, 17, 25], which gives the linear response of a mean-field ground state to neutrinos. The RPA response thus neglects clustering and is incorrect for nuclear matter at

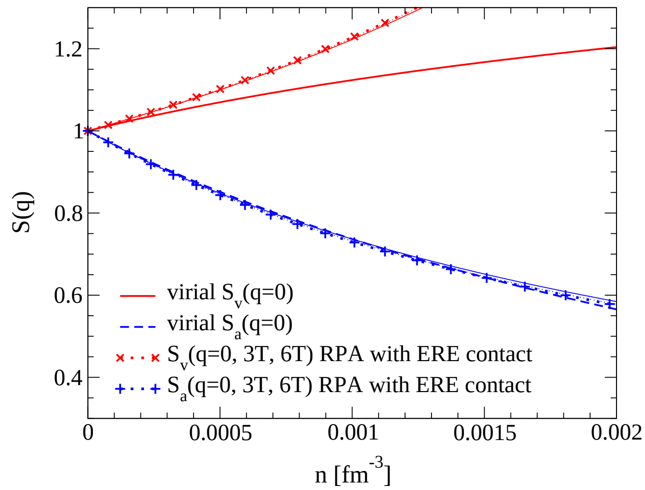

FIG. 4: (Color online) The long-wavelength virial response of neutron matter for $T = 4\,\text{MeV}$ is compared to the RPA response with effective-range expansion (ERE) contact interactions and average neutron energy $\langle E \rangle = 3T/2$.

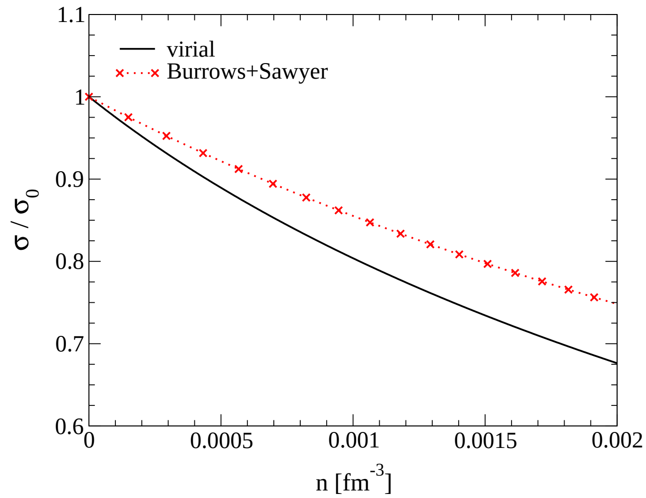

FIG. 5: (Color online) The total response of neutron matter given by the ratio of the total cross section for elastic neutrino-neutron scattering in the medium compared to free space. The results shown are for $T = 4\,\text{MeV}$ and neglect the small momentum dependence of the vector and axial response.

subnuclear densities [26]. Since there is no clustering in neutron matter, a comparison of the virial with RPA response assesses the interactions used in present RPA calculations, as well as the random-phase many-body approximation for low densities and high temperatures.

As an example, we compare our virial results to the nonrelativistic RPA calculations of Burrows and Sawyer [17], where the RPA interaction is chosen to reproduce Landau-Fermi liquid parameters for symmetric nuclear matter. We compare to the approach of Ref. [17], because these results have been used in supernova simulations [27] and they are somewhat simpler and thus more transparent than Refs. [2, 25]. Since Burrows and Sawyer do not present results for pure neutron matter, we have calculated the RPA response following Ref. [17]. For completeness, we give the necessary equations in Appendix A. For low-density neutron matter, the effective mass is well approximated by the free mass [24], and we thus use $m^*/m = 1$.

In Fig. 3, we compare the RPA results for $T = 4\,\text{MeV}$ to the virial response. We find that the RPA axial response is repulsive ($S_a < 1$) and on a qualitative level similar to the virial response. However, the RPA vector response is also repulsive, in contrast to our virial result. This is because Ref. [17] uses Landau parameters of symmetric nuclear matter for all proton fractions. In particular, Burrows and Sawyer use for the spin-independent part of the interaction $F_0 + F_0' \boldsymbol{\tau}_1 \cdot \boldsymbol{\tau}_2$, with $F_0 = -0.28$ and $F_0' = 0.95$ [17], and the density-density interaction for neutrons is thus $F_0(T=1) = F_0 + F_0' = 0.67$. This makes the incorrect assumption that induced interactions in nuclear and neutron matter are identical. For the virial coefficient b_n, the total phase shift is attractive [4]. This leads to an attractive vector response ($S_v > 1$) at low densities and low-momentum transfers. The RPA results of Refs. [2, 25] have an attractive vector response, consistent with the mean-field equation of state. However, the axial interaction of Ref. [25] is not constrained at the mean-field level and may be more poorly determined.

The RPA provides a model to study the momentum dependence of the response functions. For a neutrino with energy $E_\nu = 3T$, the maximum momentum transfer is $q_{\max} = 2E_\nu = 6T$. In addition to the long-wavelength response, Fig 3 shows the RPA results for various momentum transfers. This demonstrates that the RPA response has a very weak momentum dependence. Consequently, the long-wavelength response provides strong constraints for all relevant momentum transfers.

Next, we calculate the RPA response, when we use contact interactions that are constrained by nucleon-nucleon scattering. In order to obtain cutoff-independent results and correctly include the large scattering length and effective range at low density, it is necessary to sum particle-particle ladders and work with the T matrix (see also [28]). This leads to Landau parameters $f_0 + g_0\, \boldsymbol{\sigma}_1 \cdot \boldsymbol{\sigma}_2$ ($F_0 = m\, k_{\rm F} f_0/\pi^2$ and $G_0 = m\, k_{\rm F} g_0/\pi^2$) for the antisymmetrized interaction with

$$f_0 = \frac{2\pi/m}{1/a_{np} - m\, r_e\, E/2} \quad \text{and} \quad g_0 = -f_0 \,, \tag{27}$$

where $r_e = 2.68\,\text{fm}$ is the effective range and E denotes the relative energy. In order to make a simple estimate, we take an average relative energy $\langle E \rangle = \langle (p_1 - p_2)^2 \rangle / 4m = 3T/2$ and calculate the RPA response with these Landau parameters. The resulting vector and axial response is shown in Fig. 4. The axial response agrees nicely with our virial result, but for the vector response there is only a good agreement at low densities. The differences at higher densities could be due to using an average energy, since the vector response is more sensitive to the latter.

Finally, we show the total response of neutron matter for $T = 4\,\mathrm{MeV}$ in Fig. 5. The total response is given by the ratio of the total cross section for elastic neutrino-neutron scattering in the medium compared to free space. We neglect the small momentum dependence of the vector and axial response, and thus have $\sigma/\sigma_0 = (6g_a^2 S_a(0) + 2S_v(0))/(6g_a^2+2)$. We find for example a factor 0.72 reduction of the total response at $n = 0.0016\,\mathrm{fm}^{-3} = n_0/100$. This is 10% larger compared to the RPA response of Burrows and Sawyer.

IV. CONCLUSIONS

We have extended our virial approach to study spin-polarized neutron matter and the consistent long-wavelength response. The virial expansion is suitable to describe matter near the supernova neutrinosphere, and this work extends the virial equation of state [3, 4] to predict neutrino interactions in neutron matter. Our results include the physics of the large neutron-neutron scattering length in a tractable way. We have found that the spin virial coefficients are approximately temperature independent over a wide range. The properties of spin-polarized neutron matter and the response therefore scale with density and temperature as discussed in Ref. [4].

The virial expansion was used to make model-independent predictions for the pressure and entropy of spin-polarized matter, for the vector and axial response, and the cross section for neutrino-neutron scattering in the medium. The virial pressure and entropy of spin-polarized neutron matter are similar to Brueckner results [23], but the virial approach has a well-defined range of validity and is directly based on scattering data.

The virial equation of state predicts an attractive vector and a repulsive axial response in the long-wavelength limit at low densities. The total neutrino response is suppressed in matter compared to the response of a free neutron gas. This provides a benchmark for many-body calculations of the response functions. As an example, our results for the neutrino response disagree with the RPA response of Burrows and Sawyer [17] due to the interaction model used for the latter. The RPA was used to study the momentum dependence of the response functions. We have found a very weak dependence on momentum transfer (independent of sign and magnitude of the interaction). We therefore conclude that the long-wavelength virial response provides strong constraints at low densities for all relevant momentum transfers.

Important areas of future work are the extension of these techniques to charged-current interactions and to the neutrino response in nuclear matter [26]. In addition, a generalization of the virial expansion beyond Section II C may offer insights to the effects of multi-pair states on the long-wavelength response at low densities [15]. The third virial coefficient can be used to provide error estimates [3, 4]. For the neutrino response, an effective field theory calculation of the dominant large scattering length contributions to the third spin virial coefficients would be very useful.

Acknowledgments

We thank Isaac Vidana for providing us with the Brueckner results. This work is supported by the US Department of Energy under Grants No. DE–FG02–87ER40365 and DE–FG02–97ER41014.

APPENDIX A: RPA RESPONSE

The static structure function $S(q)$ is given in terms of the polarization function $\chi(q,\omega)$ by

$$S(q) = \frac{1}{\pi} \int d\omega \, \frac{\mathrm{Im}\,\chi(q,\omega)}{1 - e^{-\omega/T}} \,, \tag{A1}$$

where the polarization function in RPA reads

$$\chi(q,\omega) = \frac{\Pi^0(q,\omega)}{1 - v_0\,\Pi^0(q,\omega)} \,. \tag{A2}$$

The Landau interaction used by Burrows and Sawyer [17] is $v_0 = f_0 = 1.76 \cdot 10^{-5}\,\mathrm{MeV}^{-2}$ for the density response and $v_0 = g_0 = 4.50 \cdot 10^{-5}\,\mathrm{MeV}^{-2}$ for the spin response. The real and imaginary parts of the free polarization $\Pi^0(q,\omega)$ are derived in the Appendix of Ref. [17],

$$\mathrm{Re}\,\Pi^0(q,\omega) = \frac{m^2}{2\pi^2 q\beta} \int\limits_0^\infty \frac{ds}{s} \ln\!\left[\frac{1+e^{\beta\mu-(s+Q)^2}}{1+e^{\beta\mu-(s-Q)^2}}\right] + \omega \to -\omega \,, \tag{A3}$$

$$\mathrm{Im}\,\Pi^0(q,\omega) = \frac{m^2}{2\pi q\beta} \ln\!\left[\frac{1+e^{\beta\mu-Q^2}}{1+e^{\beta(\mu-\omega)-Q^2}}\right] , \tag{A4}$$

with $Q = \sqrt{m\beta/2}\,(-\omega/q + q/(2m))$. Finally, the density is given by

$$n = 2 \int \frac{d^3p}{(2\pi)^3} \frac{1}{1+e^{\beta(p^2/(2m)-\mu)}} \,, \tag{A5}$$

which determines the chemical potential for Eqs. (A3,A4).

[1] A. Mezzacappa, Annu. Rev. Nucl. Part. Sci. **55** (2005) 467.

[2] S. Reddy, M. Prakash, J.M. Lattimer and J.A. Pons,

Phys. Rev. **C59** (1999) 2888.
[3] C.J. Horowitz and A. Schwenk, Nucl. Phys. **A776** (2006) 55.
[4] C.J. Horowitz and A. Schwenk, Phys. Lett. **B638** (2006) 153.
[5] S. Kowalski *et al.*, nucl-ex/0602023.
[6] M. Costantinit, A. Ianni and F. Visanni, Phys. Rev. **D70** (2004) 043006.
[7] C. Lunardini and A.Y. Smirnov, Astropart. Phys. **21** (2004) 703.
[8] A. Burrows, S. Reddy and T.A. Thompson, astro-ph/0404432.
[9] C.J. Horowitz, Phys. Rev. **D65** (2002) 043001.
[10] E. Beth and G.E. Uhlenbeck, Physica **4** (1937) 915.
[11] K. Huang, Statistical Mechanics, Wiley N.Y., Second Edition (1987), p. 224-227.
[12] A. Pais and G.E. Uhlenbeck, Phys. Rev. **116** (1959) 250.
[13] P.F. Bedaque and G. Rupak, Phys. Rev. **B67** (2003) 174513.
[14] G. Rupak, nucl-th/0604053.
[15] Olsson and C.J. Pethick, Phys. Rev. **C66** (2002) 065803; G.I. Lykasov, E. Olsson and C.J. Pethick, Phys. Rev. **C72** (2005) 025805.
[16] L.D. Landau and E.M. Lifschitz, Statistical Physics, Pergamon N.Y., Second Edition (1969), Eq. (114.14).
[17] A. Burrows and R.F. Sawyer, Phys. Rev. **C58** (1998) 554.
[18] V.G.J. Stoks, R.A.M. Klomp, M.C.M. Rentmeester and J.J. de Swart, Phys. Rev. **C48** (1993) 792; see also NN-OnLine, http://nn-online.org.
[19] T.-L. Ho and E.J. Mueller, Phys. Rev. Lett. **92** (2004) 160404.
[20] T.-L. Ho, Phys. Rev. Lett. **92** (2004) 090402.
[21] J.E. Thomas, J. Kinast and A. Turlapov, Phys. Rev. Lett., **95** (2005) 120402.
[22] B. Friedman and V.R. Pandharipande, Nucl. Phys. **A361** (1981) 502.
[23] I. Bombaci, A. Polls, A. Ramos, A. Rios and I. Vidana, Phys. Lett. **B632** (2006) 638; I. Vidana, private communication.
[24] A. Schwenk, B. Friman and G.E. Brown, Nucl. Phys. **A713** (2003) 191.
[25] C.J. Horowitz and M.A. Perez-Garcia, Phys. Rev. **C68** (2003) 025803.
[26] C.J. Horowitz and A. Schwenk, in preparation.
[27] R. Buras, M. Rampp, H.-Th. Janka and K. Kifonidis, astro-ph/0507135.
[28] A. Schwenk and C.J. Pethick, Phys. Rev. Lett. **95** (2005) 160401.
[29] The second virial coefficient b_n follows with $\delta^{\rm tot}(E)/2$ instead of $\delta_1^{\rm tot}(E)$ in Eq. (9) [4].